# Misfit dislocation network at the Ag/MgO(001) interface: A grazing-incidence x-ray-scattering study

G. Renaud,* P. Guénard, and A. Barbier
*CEA-Grenoble, Département de Recherche Fondamentale sur la Matiére Condensée/SP2M/IRS, 17, rue des Martyrs, 38054 Grenoble Cédex 9, France*
(Received 18 November 1997; revised manuscript received 23 March 1998)

The misfit dislocation network at the Ag/MgO(001) interface has been investigated by grazing incidence x-ray diffraction on Ag films of different thicknesses, between 100 and 1500 Å deposited at room temperature by molecular beam epitaxy on MgO(001) surfaces with different step densities. They were analyzed after growth and after annealing at increasing temperatures. A square network of edge dislocations is found to release the 3% lattice misfit between Ag and MgO. The dislocation lines are found oriented along ⟨110⟩ directions, with $a/2[110]$ Burgers vector. Quantitative analysis shows that the substrate is deformed according to the elasticity theory. The as-grown Ag films contain stacking faults and twins, in amounts that increase with increasing substrate surface step density. Annealing the film at low temperature 300 °C eliminates the stacking faults. Annealing at higher temperatures induces a recrystallization of the Ag epilayers, as well as an improved ordering of the dislocation network. For increasing temperatures, the period of the dislocation network instantaneously adapts to the actual lattice parameter misfit. After cooling, a large residual deformation is found in Ag, which is smaller when the substrate step density is larger. This is interpreted in terms of an energetic barrier for the nucleation of misfit dislocations. [S0163-1829(98)07532-8]

## I. INTRODUCTION

Metal/ceramic interfaces are involved in many technological materials: electronic packaging, catalysis, protective coatings, thin-film technology, composites, or glass industry. Many of their electrical, thermal, or mechanical properties depend on the atomic structure of the metal/ceramic interface they contain. Thus, in recent years, the structure of metal/oxide interfaces has made a number of new experimental and theoretical contributions.[1] Despite this interest, little is known about metal-oxide adhesion because of the complex nature of the interactions involved between these dissimilar materials. The Ag/MgO(001) system is one of the most simple metal/oxide interfaces because both constituting materials have a cubic lattice, the epitaxial relationships are known to be cube on cube, the lattice parameter misfit is small, and chemical and charge transfer contributions to bonding are negligible. For these reasons, it has been chosen by many theoreticians as a model metal/oxide interface to refine the theoretical models.[2] However, theoreticians normally neglect the lattice parameter misfit in their calculations, while it is these interfacial defects that play a dominant role on the energetic of the interface. These defects could be of different nature: dislocations, stacking faults, twins, rotation of the epilayer with respect to the substrate, roughness, etc.

From the point of view of elasticity, the relaxation is governed by the lattice parameter misfit $f$ defined by $f=(a_f-a_s)/a_s$, where $a_f$ and $a_s$ are respectively the film and substrate lattice parameters. For small values of $f$ ($<10\%$), semicoherent interfaces are often observed, in which the lattice parameter misfit is accommodated by localized and ordered misfit dislocations.[3] When $f$ is larger, the misfit dislocation density becomes so large that they cannot remain localized and organized: the interface is said to be ''incoherent.'' There are, however, numerous exceptions. For instance, the Pd/$\eta$-$Al_2O_3$(111),[4] Au/MgO(001),[5] Cu/$Al_2O_3$ (Ref. 6) and the Ag/CdO (Ref. 7) interfaces are incoherent with $f=2.7\%$, 3%, 10% and 14%, respectively, while the Au/$ZrO_2$(111) interface is semicoherent with $f=22\%$.[4]

For the Ag/MgO(001) interface, $f=-2.98\%$. Hence, a semicoherent interface is expected. Ordered, localized interfacial misfit dislocations have been observed by HRTEM.[8] This study concluded that the dislocation lines were oriented along ⟨100⟩, which could only be explained by the coexistence of two epitaxial sites for silver in the regions of ''good match'' between the Ag film and the MgO substrate. This result was very surprising because all theoretical calculations of the epitaxial site performed so far[2] concluded one site, above O ions, was preferred. This was also our experimental conclusion,[9] from a previous grazing incidence x-ray scattering[10] (GIXS) investigation of the early stages of growth of Ag on MgO(001). In addition, the HRTEM samples were extremely difficult to prepare,[8] so that only (100) and no (110) cross section could be observed. Since the (100) cross section was blurred, the conclusion regarding the orientation was controversial.[11] To the best of our knowledge, no plane view transmission electron microscopy experiment has ever been performed in order to identify the orientation of the dislocation network. This is probably due to the difficulty to prepare sample because of the very weak interfacial bonding. These considerations led us to carry out an investigation of this dislocation network x-ray diffraction on this interfacial superlattice, using grazing incidence conditions, as was successfully in the case of a semicoherent semiconductor interface, GaSb(001)/GaAs(001).[12]

It will be shown that GIXS allows a clear determination of the dislocation network orientation. In addition, it provides new information on the residual deformation as a function of thickness and on the effect of annealing an interface

 

between materials having different thermal expansion coefficients. The evolution of the residual deformation after anneals and its dependency upon the step density of the substrate will be discussed.

Before presenting the results, a few preliminaries will be given in simple terms in order to describe the different possible network orientations in the Ag/MgO(001) interface, and how they can be distinguished by x-ray scattering. The experimental conditions and results are next described, showing x-ray-scattering features from the dislocation network, the stacking faults and twins in the Ag film, and the substrate steps. The effect of annealing the samples at increasing temperatures is next illustrated, and a well-ordered interface is selected for a quantitative comparison with calculation. The dependence of the residual deformation as a function of annealing temperature and substrate miscut is finally discussed.

## II. BACKGROUND

Consider two crystals of different lattice parameter with the same crystallographic structure, which are not deformed, and in epitaxy. Zones of ''good match'' and ''poor match'' alternate parallel to the interface, forming a network[13] called coincidence-site lattice (CSL),[14] or *O* lattice, defined as the smallest lattice that is common to the two primitive ones. Its period $\Lambda$ is given by $\Lambda = a_f/|f| = a_s(1-|f|)/|f|$. In the ''poor match'' regions, the atoms are subject to coherency forces that tend to reorganize the structure to form a network of misfit dislocations of period $\Lambda$. In the case of the Ag/MgO(001) interface, according to the different possible epitaxial sites, different CSL may be considered. Because of the symmetries of the MgO(001) plane, the Ag atoms may sit either above oxygen ions of the substrate, or above magnesium ions, or in between, above the octahedral site, with two possible variants.[8] If they sit above only one of the possible epitaxial site, a square CSL oriented along $\langle 110\rangle$ directions is obtained, of 97 Å periodicity. If there are two equivalent epitaxial sites, for instance, O and Mg, or the two variants of the octahedral site, then a square network oriented along $\langle 100\rangle$ directions is obtained, of 69-Å periodicity, $\sqrt{2}$ times smaller than for the $\langle 110\rangle$ CSL. This is the network suggested by the previous HRTEM study.[8]

Since the misfit dislocations are ordered, they may be observed by x-ray diffraction. The dislocation network yields satellites that are only intense close to Bragg peaks. As illustrated in Fig. 1, it is possible to distinguish between the $\langle 100\rangle$ and $\langle 110\rangle$ dislocation networks by performing x-ray diffraction along the $(h00)$ and $(hh0)$ directions of the reciprocal space. Along the $(hh0)$ direction, the satellite periodicity is double in the case of a $\langle 110\rangle$ CSL with respect to the $\langle 100\rangle$ case. Hence simple GIXS measurement should allow distinguishing unambiguously between these two possibilities.

## III. EXPERIMENT

Seven samples were studied, differing either by the substrate preparation, by the conditions of Ag deposition, or by the silver film thicknesses. Different GIXS setups were used for the experiments. These experimental conditions, described below, are summarized in Table I.

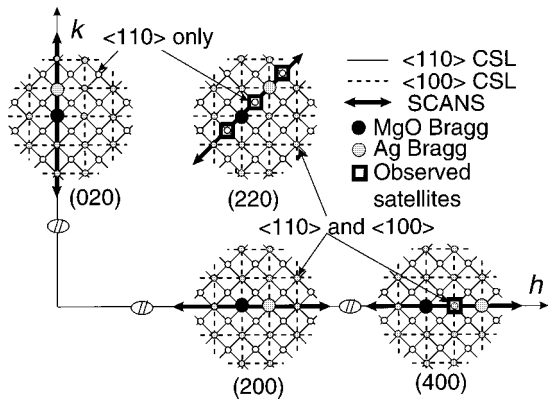


FIG. 1. Schematic representation of the $(h\ k\ 0)$ interfacial plane of the reciprocal lattice of the Ag/MgO(001) interface with an interfacial network of misfit dislocations. Large black and gray disks respectively represent the MgO and Ag Bragg peaks. The reciprocal lattices of the two possible interfacial misfit dislocation networks are also shown as grids, with continuous lines for the $\langle 110\rangle$ CSL, and dashed line for the $\langle 100\rangle$ one. The locations of satellites from the interfacial network are represented as gray disks for the satellites that are common to the two CSL, and as open circles for those satellites that pertain only to the $\langle 110\rangle$ CSL. The experimental radial scans performed on the different samples are also indicated. A scan along the (110) reciprocal direction, between the MgO(220) and Ag(220) Bragg peaks, should allow unambiguous distinction between the two possible network orientations.

### A. Samples

In order to directly compare the x-ray scattering results with the previous HRTEM ones,[8] most samples were prepared by the same group,[15] using the same MBE apparatus,[16] and under conditions as close as possible to the preparation conditions of HRTEM samples. The MgO(001) substrates, $10\times 10\times 0.5$ mm$^3$, were prepared by cleavage of commercial bars. They were subsequently annealed during 4 h at 850–900 °C in ultrahigh vacuum (UHV), before MBE deposition of a ~200-Å-thick MgO(001) buffer layer with the substrate held at 600 °C. Silver was deposited at room temperature with typical rates between 0.1 and 1 Å/s. For all these samples, large miscut values, typically of the order of 2°, were always found during the GIXS measurements, which may be related to the cleavage process.

We have developed a procedure, described in detail elsewhere,[17] to obtain well-oriented, clean and extremely flat MgO(001) surfaces. The $15\times 15\times 0.5$-mm$^3$ MgO single crystals, oriented $(001)\pm 0.1°$, supplied by Sumitomo, were first annealed in air at 1500 °C for 2 days. They were next *in situ* ion bombarded at 1550 °C. To ensure the surface stoichiometry, the sample was finally annealed for 15 min at 700 °C in an oxygen partial pressure of $10^{-4}$ mbar. The resulting surface has a rms roughness of 2.4 Å over lateral length scales between 1 Å and 1 $\mu$m, with very wide atomically flat terraces.[17] On these substrates, the Ag/MgO(001) interfaces were characterized *in situ* by GIXS during Ag deposition, from the very early stages up to thicker films.[18] The substrate was held at room temperature, and Ag was deposited from a Knudsen cell, at a rate of 0.36 Å/min. We will present here the results obtained on a 1300-Å-thick film.

TABLE I. The different Ag/MgO(001) interfaces studied by GIXS: thickness of the Ag film, miscut value, determined during the GIXS experiments, synchrotron beamline and apparatus used for the GIXS experiment, and angular acceptance of the detector. The last sample (F) was prepared at the ESRF, in the D32 SUV ultrahigh vacuum chamber.

| Label | Ag thickness | Miscut | Beamline/ Diffractometer | Detector acceptance mrad(⊥)×mrad(∥) |
|---|---|---|---|---|
| A | 100 Å | 2±0.5° | LURE-W21 | 5×5 |
| B | 200 Å | 2±0.5° | LURE-W21 | 5×1 |
| C | 1500 Å | 2±0.5° | ESRF-D32/Multitechnic | 10×2 |
| C | 1500 Å | 2±0.5° | ESRF-ID13/W21 | 25×2 |
| D | 1500 Å | 2±0.5° | ESRF-ID32/W21 | 5×1 |
| E | 1500 Å | 3±0.5° | ESRF-ID32/W21 | 5×1 |
| F | 1300 Å | <0.1° | ESRF-D32/Multitechnic | 5×1 |

### B. GIXS experiments

Two GIXS diffractometers were used, on different synchrotron beamlines of the LURE (Laboratoire pour l'Utilisation du Rayonnement Electromagnétique, Orsay, France) and the ESRF (European Synchrotron Radiation Facility, Grenoble, France). The first one, called W21, has been described in detail elsewhere.[19] The vertical geometry was used, with the associated UHV chamber, equipped with Be windows, and with a radiative heating furnace reaching 900 °C. It was used on the W21 beamline of LURE,[19] as well as on the ID13 and ID32 beamlines[20] of the ESRF. The ''Multitechnique'' diffractometer of the French CRG/IF beamline BM32 (Ref. 20) of the ESRF was also used, with a small high vacuum chamber equipped with a 360° opening beryllium window. The detector angular acceptance was defined by two pairs of slits, in both directions. The angular resolutions are reported in Table I for the different GIXS measurements. All measurements were performed with an x-ray monochromatic beam of 18-keV energy. The incident angle $\alpha$ with respect to the surface was chosen to maximize the intensity of the dislocation satellites. For the thin Ag films (~100–200 Å), this amounted to ~1.5 times the critical angle for total external reflection $\alpha_c$ of Ag. For thick films, the optimum $\alpha$ value is $\sim 2\alpha_c$, because most of the scattering by the dislocation network arises from a buried region, close to the interface. The optimal Ag thickness, for which the best ratio of satellites over Ag Bragg peaks intensities is obtained, is of the order of 1300 Å.

Throughout the whole paper, the location of measurements is described by the reciprocal lattice units (r.l.u.) $h$, $k$, and $l$ in the reciprocal space of the MgO(001) substrate, of lattice parameter $a = 4.2117$ Å. The coordinate $l$ is perpendicular to the Ag/MgO(001) interface.

## IV. EXPERIMENTAL RESULTS

### A. Interfacial dislocation network

The in-plane measurements performed on the thin layers *A* (100-Å-thick Ag film) and *B* (200-Å-thick Ag film), are reported in Fig. 2. Along the $(hh0)$ direction, a shoulder is present around $h = 2.023$ for sample *A*, and a clear satellite can be seen for sample *B*, located at $h = 2.026$, between the MgO crystal truncation rod[21] (CTR) and the Ag peak. This unambiguously demonstrates that the dislocation network is of ⟨110⟩ orientation.

Because the coalescence is not complete for these thin samples, the Ag film structures are fairly disordered. In order to perform more quantitative measurements, 1500-Å-thick samples (*C*, *D*, and *E*) were investigated. These samples were better ordered, and the ⟨110⟩ orientation of the Ag film was confirmed. However, on these substrates with a significant miscut, a large background of diffuse scattering is present in the region of the Bragg peaks. As clearly demonstrated on MgO(001) surfaces obtained by cleavage from a MgO bar,[17] which has a large density of steps, these diffuse scattering contributions arise from the lateral step-step correlation. A contribution is found below the MgO peak because of the substrate steps, and a second below the Ag peak, because the substrate steps are replicated in the Ag film at the interface.

To avoid the background induced by steps, similar measurements were performed on a Ag film deposited on an especially prepared MgO(001) substrate, with a very low step density (sample F). The film thickness, of 1300 ±20 Å, was determined by x-ray reflectivity, which also yielded an average density of 9.8 g/cm$^3$ for the Ag film, instead of 10.5 g/cm$^3$ for pure Ag. This corresponds to the presence of ''holes'' covering 10% of the sample area, as confirmed by scanning electron microscopy (SEM).

Figure 3 shows the $(h\ h\ 0.1)$ scan performed on this sample. The background below the main peaks is significantly smaller than for miscut substrates (not shown), resulting in a fivefold enhancement in the satellite over back-

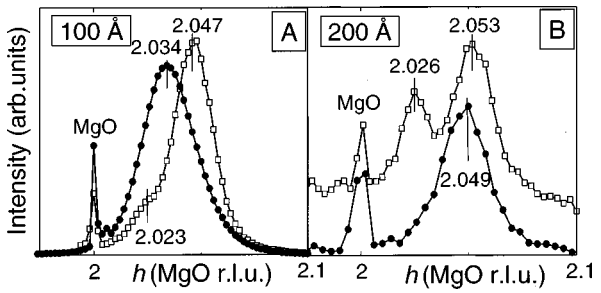


FIG. 2. Radial scans around the (200) (black disks) and (220) (open squares) Bragg peaks of Ag and MgO for samples A (100-Å-thick Ag film) and B (200-Å-thick Ag epilayer). The peaks positions are also reported. Note the satellites along the $(hh0)$ directions.

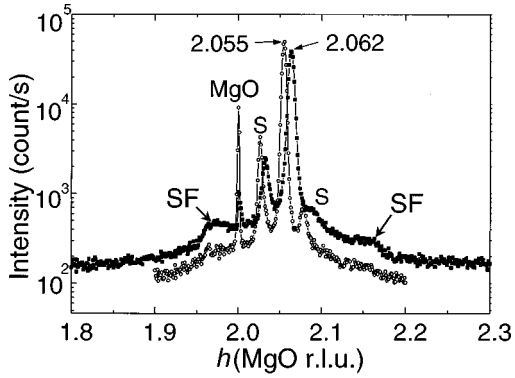


FIG. 3. Radial scan along the ($h$ $h$ 0.1) direction around the (220) Bragg peak for sample *F*, before (filled squares) and after (open circles) annealing up to 770 °C. The measurements were performed at room temperature. Satellites of diffraction by the interfacial dislocation network are denoted *S*. On this sample, which is flat and has a very small residual miscut ($<0.1°$), the background emanating from step-step scattering is negligible. Another source of scattering is present in the form of shoulders, shown by arrows. They are symmetrical with respect to the Ag peak, and are due to stacking faults (SF) in the Ag film, yielding rods of scattering along the ⟨111⟩ directions.

ground intensity ratio. Two satellites are clearly visible, confirming the ⟨110⟩ orientation of the dislocation network on this thick sample.

### B. Stacking faults and twins

On this flat sample, another kind of diffuse scattering is observed (Fig. 3) that cannot be attributed to the interfacial dislocation network, nor to interfacial steps. It is made of two shoulders, symmetric with respect to the Ag peak. As shown in Fig. 4 on large radial scans taken at room temperature before annealing on sample *D*, the separation between these two peaks increases with $l$, in such a way that they are aligned on rods emanating from the Ag Bragg peak located at (2.061 2.061 0.04), and aligned along the (111) and (111) directions. One possible explanation of these ⟨111⟩ rods could be crystal truncation rods[21] arising from (111) facets of the Ag surface, since for Ag, the (111) surface orientation is energetically favored with respect to the (001) one. However, an estimation of the intensity scattered by such facets shows that the surface should be completely decomposed into (111) facets to reproduce the observed rods. The intense Ag(2.061 2.061 $l$) CTR (Fig. 4) demonstrates that most of the surface is of (001) orientation.

These rods rather originate from stacking faults along (111) planes.[22,23] These faults can be described by two semi-infinite crystals, related to each other by a (2/3 1/3 1/3) translation. Because of the phase shift between the two crystals, the CTR from the two (111) planes around the fault do not cancel each other. The residual intensity consists of rods oriented along {111} directions, extending from each Ag Bragg peak.

Another interesting feature seen in Fig. 4 is the peak measured around (2.404 2.404 0.35), which can be attributed to another kind of growth fault: the twins, corresponding to two crystals of reverse fcc stacking, with a mirror plane at the

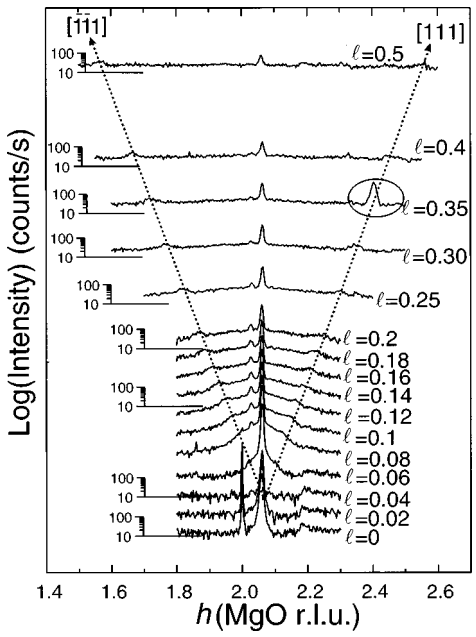


FIG. 4. Radial scans ($hhl$) around $h=2$ on sample D (1500-Å-thick Ag film) at room temperature, before annealing. A vertical translation, proportional to $l$, has been introduced between the different scans. In addition to the MgO and the Ag CTR's and to the dislocation satellite rod, there are additional rods of scattering, oriented along the ⟨111⟩ directions, and crossing the relaxed Ag peak around $l\sim0.04$. These rods are due to stacking faults in the silver film. The peak around $h=2.404$ and $l=0.35$ arises from twinned Ag domains. The shift in $l$ (0.04) of the origin of the stacking fault rods is due to refraction in the Ag film.

fault location. This structure no longer produces rods, but produces additional peaks[22,23] arising from the twinned Ag crystal. Around the (220) Ag Bragg peaks, these ''twin'' peaks appear at (220)+1/3(111) and (220)+2/3(111),[22] in reciprocal lattice units of Ag. Hence, these data show that, in addition to the interfacial dislocation network, growth faults are present within the Ag thin film, mainly stacking faults and twins along (111) planes, which are likely to occur during coalescence of neighboring islands of different stacking.

### C. Effect of annealing

In order to get further information on the interfacial dislocation network, quantitative measurements of several diffraction satellites are required. This implies samples with a better ordered dislocation network yielding more satellites of larger intensity on one hand, and with as small as possible background below these satellites on the other hand. A mandatory condition for the last requirement to be met is to start with a substrate surface with the lowest possible step density. In order to meet the first requirement, the samples were annealed at different temperatures.

Figure 3 illustrates the effect of annealing on the silver film. The background due to the stacking faults decreases tremendously, the Ag peak as well as the main satellite increase and become narrower, and additional satellites appear, both on the right of the Ag peak and on the left of the MgO one. Several experiments have thus been performed to characterize in more detail the evolution of the Ag film as well as

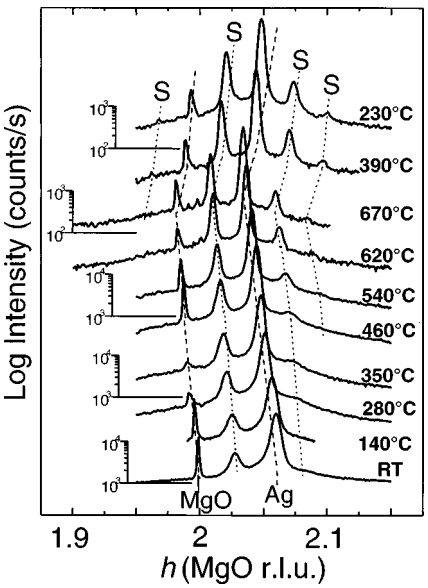


FIG. 5. Radial scans along the ($h$ $h$ 0.1) direction around the (220) Bragg peak for sample C, at different temperatures during heating followed by cooling back to room temperature. Satellites from the interfacial dislocation network are labeled ''$S$.''

the dislocation network crystalline quality as a function of annealing at increasing and decreasing temperatures.

Because the MgO thermal expansion parameter of $13.5 \times 10^{-6}$ $K^{-1}$ is smaller than the Ag one of $19.0 \times 10^{-6}$ $K^{-1}$ (Ref. 24), the lattice parameter misfit $f$ decreases with increasing temperature. Hence, at equilibrium, the period of the dislocation network is expected to increase with temperature, resulting in a larger separation between dislocations at higher temperatures. Figure 5 shows the evolution of the ($h$ $h$ 0.16) scan taken on sample $C$ during a cycle of annealing at increasing and decreasing temperatures. During heating, all peaks shift toward smaller $h$ values because of thermal expansion. The experimental evolution of the lattice parameter misfit with temperature was deduced, both during heating and during cooling, from the exact positions of the MgO and Ag Bragg peaks.

Several features can be inferred from Fig. 5. Firstly, the main satellite, at (2.031 2.031 0.16) on the as-grown sample, always remains exactly centered in between the MgO and Ag peaks, whatever the temperature. This indicates that, when the misfit varies, the period of the dislocation network changes in order to be exactly on the CSL. Secondly, annealing clearly induces a recrystallization of the Ag thin film, as revealed by a narrowing of the Ag peak in both radial and transverse directions. Transverse measurements of different orders of diffraction by the Ag film reveal that the crystalline quality is limited by a finite mosaic spread, which decreases from ~0.25° down to ~0.15° after annealing. Thirdly, annealing also dramatically improves the ordering of the dislocation network. Around 350 °C, the second satellite on the right of the Ag peak becomes clearly visible, and two other satellites appear around 620 °C. All peaks are equidistant, the satellites' positions being defined by the periodicity of the dislocation network, itself related to the separation between the MgO and Ag peaks. With increasing temperature, all satellites increase and narrow faster than the Ag peak. After annealing at 230 °C, the ratio between the main satellite and the Ag peak intensities is already ~50% larger than on the as-grown sample, while it is 80% larger after annealing at 670 °C. At all temperatures, the transverse width of the dislocation satellites is exactly equal to that of the Ag peaks, which shows that the crystalline order of dislocations is also limited by the Ag mosaic spread.

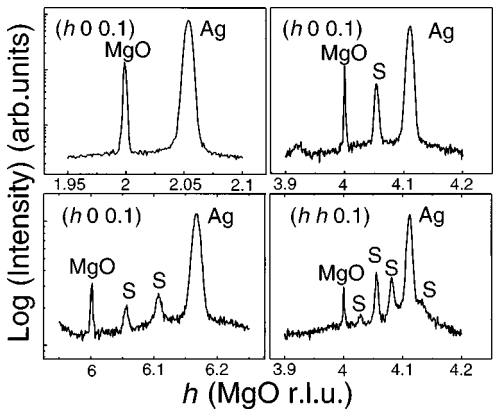


FIG. 6. Radial scans on the ''flat substrate'' sample (F) after high-temperature annealing up to 770 °C. The diffraction satellites from the interfacial network of misfit dislocations are labeled ''$S$.'' The scan around the (220) reflection is shown in Fig. 3.

Another remarkable feature is that the dramatic reduction of the diffuse scattering due to stacking faults starts at low temperature, around 250 °C, and is almost complete at 300 °C. This result could be expected because the formation of stacking faults is known to be easy in silver. It may be of use in order to grow fault-free thick buffer silver layers on MgO(001), for instance, in view of performing GIXS measurements on a good starting Ag(001) surface, avoiding the large thermal diffuse scattering of Ag(001) single crystal surfaces.[25]

### D. Quantitative measurements of the dislocation network

Quantitative measurements of all measurable dislocation satellites around the (200), (400), (600), (220), and (440) locations were performed at room temperature (RT) on the flat sample ($F$) after it had been annealed at 770 °C. Both radial (Fig. 3 and Fig. 6) and transverse scans were performed, for a perpendicular momentum transfer value of $l = 0.1$, which yielded the best signal over background ratio. On this sample, all in-plane peaks had a transverse full width at half maximum of $0.10° \pm 0.02°$, thus limited by the Ag film mosaic spread. They were integrated both radially and transversely, and corrected for the active area, monitor normalization, polarization and appropriate Lorentz corrections. The measured diffraction pattern is reported in Fig. 7.

## V. ANALYSIS, INTERPRETATION, AND DISCUSSION

### A. Orientation of the dislocation network

All the above data demonstrate that, for very different film thickness, preparation conditions or substrate step density, the dislocation network is always oriented along ⟨110⟩ directions, with Burgers vectors of the $a/2[110]$ type. Moreover, annealing experiments show that this orientation and Burgers vectors are preserved when heating the sample. This

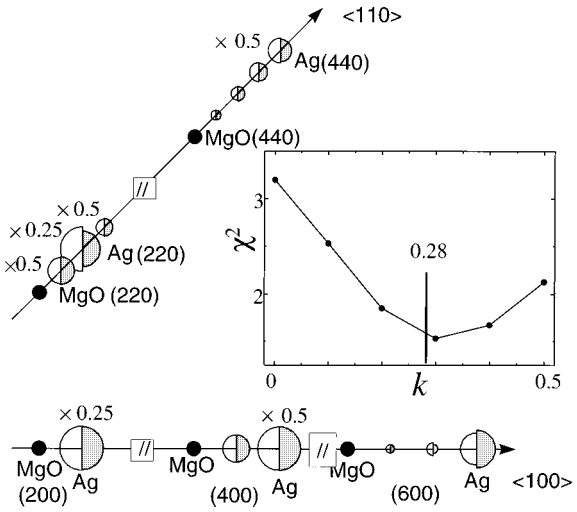


FIG. 7. Diffraction pattern of the Ag/MgO(001) interface measured on the ''flat substrate'' sample (F) after high-temperature annealing up to 770 °C, in the $(h\ h\ 0.1)$ plane. The experimental structure factors, measured by radial and rocking integration followed by area, Lorentz and polarization corrections, are represented as open half circles whose radius is proportional to the structure factor (and hence the area is proportional to the intensity) on the left of each peak location. On the right are represented (gray half disks) the calculated structure factors corresponding to the best fit (see text), with a ratio $k=0.3$ or the shear modulus of Ag over the shear modulus of MgO. The inset shows the evolution of the agreement factor $\chi^2$ as a function of this ratio. The best fit is obtained for the value of $k=0.3$, which is close to the actual value (0.28) deduced from the tables.

$\langle 110\rangle$ orientation is consistent with the uniqueness of the epitaxial site (above oxygen ions of the substrate) during the initial stages of epitaxy, that we have demonstrated earlier by GIXS.[9]

This conclusion stands in contradiction with the $\langle 100\rangle$ orientation deduced from a previous HRTEM investigation.[8] Since HRTEM is a method of choice to investigate dislocations, the possible reasons leading to a mistaken interpretation must be examined. Firstly, HRTEM cross sections were observed only in the (100) plane, in which both kinds of networks yield similar contrast,[11] and no (110) cross section was available. These images were blurred, which is expected for a $\langle 110\rangle$ orientation, but which should not be the case if the network orientation was really $\langle 100\rangle$.[11] Secondly, according to the authors themselves, the preparation of thin samples adapted for HRTEM was extremely difficult, mainly because of the weak adhesion energy of this interface. It is thus possible that an initially $\langle 110\rangle$-oriented network could have evolved during sample preparation. Since the typical thickness of an HRTEM specimen is $\sim$100 Å, i.e., comparable to the separation between dislocations, the lattice parameter relaxation perpendicular to the cross section could be performed at the edges. For a (010) cross section, it could thus be possible that, during preparation, an $a/2[110]$ dislocation would dissociate into two other dislocations: $a/2[100]+a/2[010]$. The dislocation lines parallel to the section could be eliminated at the edges, leaving only the perpendicular dislocations to relax the remaining stress parallel to the section. Another possible scenario that was originally thought was that the reorientation of the dislocation could result from heating of the sample, which could have occurred during ion beam milling down to the appropriate thickness. However, the observation of the stability of the network orientation during heating up to elevated temperature rules out this possibility.

Note that the $a/2[100]$ Burgers vector is not a vector of the fcc Bravais lattice of Ag, and is thus by definition a partial dislocation, associated with a stacking fault in the (100) plane. Since this stacking fault is not a ''natural'' stacking fault of Ag it must have a high energy, and thus a small probability.

### B. Quantitative analysis of the dislocation network

One important goal of our investigation was to quantitatively compare the experimental results with calculated intensities, in order to test the ability of the available models to calculate the main characteristics of the dislocation network, as probed by x-ray diffraction.

According to the respective substrate and film elastic properties, the core of the dislocations may be located at a given distance away from the interface.[26,27] A calculation similar to that performed in the $Nb/Al_2O_3$ case[27] was done for the Ag/MgO(001) interface, yielding the equilibrium distance $\lambda_0 \approx 1.2 \pm 0.3b$ between the dislocation core and the substrate surface, where $b$ is the modulus of the Burgers vector. Since this value is expected to be overestimated by a factor of 2,[27] one can conclude that, in the present case, the dislocations are located at the interface, which is also the experimental HRTEM conclusion.[8] In order to calculate the displacements induced by the dislocations, we can thus resort to a model in which the dislocation cores are located at the interface.

An analytical model,[28,29] developed in the framework of linear elasticity in a continuous and isotropic medium was used to compute the complete 3D displacement field. All atomic positions, within a Ag(001) film of finite thickness in semicoherent epitaxy with MgO(001) were calculated for different values of the ratio $k=\mu_{Ag}/\mu_{MgO}$ of the shear modulii of Ag and MgO. The structure factors of all main satellites were next computed. They were fitted to the data with only three parameters: a scale factor common to all satellite peaks, a different scale factor for Ag Bragg peaks, in order to take into account the finite thickness simulated, and a Debye-Waller factor taken identical for all atoms. The $\chi^2$ agreement factor was found very sensitive to the ratio $k$, as shown in the inset of Fig. 7. The best agreement is obtained for $k=0.3$, which yields $\chi^2=1.5$, very close to the ideal value of 1. For a rigid substrate $(k=0)$, a much worse agreement $(\chi^2=3.2)$ is obtained. Indeed, if this approximation is justified for very thin films,[30] it almost certainly breaks for the thick films investigated here. The calculated structure factors for $k=0.3$ are reported in Fig. 7 for comparison with the experimental ones, which confirms the quality of the agreement, for all measured peaks. The optimal Debye-Waller factor value of $\sqrt{\langle u\rangle^2}=0.15$ Å is slightly larger than in bulk silver (0.1 Å), which is probably representative of static disorder.

This simulation shows that the substrate is effectively deformed by the Ag film, and this deformation significantly contributes to the experimental data. The best agreement is

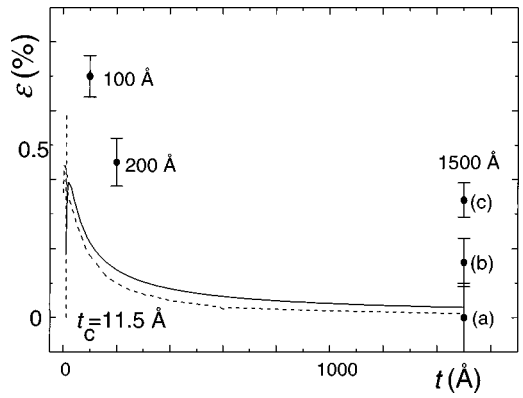


FIG. 8. Calculated residual deformation $\epsilon$ of the Ag epilayer as a function of its thickness $t$, according to an approximate calculation (continuous line) (Ref. 31) and to a more precise numerical calculation (dashed line) (Ref. 28). Experimental values with error bars are also reported for (a): 100-Å, 200-Å, and 1500-Å-thick samples before annealing; (b) the 1500-Å-thick ''miscut'' samples after annealing, and (c): the 1300-Å sample with a flat interface (sample F) after annealing.

actually found for a value very close to the tabulated value ($k=0.28$), which clearly demonstrates that the theory of elasticity is well adapted to calculate the deformation field in both the substrate and the film. It is also well adapted to calculate the properties of the interface, without invoking a weaker ''effective interfacial modulus.'' [3] These results validate the choice of this quantitative model, and show that a numerical simulation that would be required to better describe the detailed structure of the core of the dislocation is not necessary to reproduce these experimental data. This actually implies that for this $l$ value, the scattered intensity is mainly sensitive to atomic displacement far from the dislocation cores, rather than to the dislocation core itself. Further measurements of the dislocation satellites as a function of the perpendicular coordinate $l$ would be required to determine if, for large $l$ values, x-ray scattering could be sensitive to the atomic structure of the dislocation cores.

### C. Residual deformation of the Ag film, effect of annealing

For almost all samples, whatever the film thickness and the annealing history, a residual deformation remains, which depends upon the thickness of the film, the density of steps on the substrate and the state, as grown or annealed, of the sample.

The residual deformation measured on the different samples before and after annealing are compared in Fig. 8 to the result of an elastic calculation of the residual deformation[28,31] as a function of the film thickness. Whatever the step density and preparation conditions, all 1500-Å-thick as-grown Ag films are nearly fully relaxed. They are close to the equilibrium conditions, since the residual deformation is that predicted by the linear elasticity theory. By contrast, thin films as well as annealed films always have experimental residual deformations larger than the calculated ones.

For the 100-Å- and 200-Å-thick samples (Fig. 3), the residual deformation is always larger in the ⟨100⟩ direction than in the ⟨110⟩ direction, and this difference of residual deformation decreases with increasing thickness. This is linked to the 3D character[18] of the growth of Ag on MgO(001), with nucleation, growth, and coalescence of Ag islands. The 100-Å- and 200-Å-thick films have not yet fully coalesced, and are thus composed of large islands separated from each other. Since for 3D islands, the deformation, and thus the stress, is imposed only on the atomic plane that is in contact with the substrate, the relaxation may partly proceed on the edges. The observed nonbiaxial deformation could then be related to the elastic anisotropy of Ag. Indeed, by using the elasticity theory, very different values of the Young modulus, $E_{100}=44$ GPa and $E_{110}=84$ GPa, are found along the ⟨100⟩ and ⟨110⟩ directions. Ag is thus softer in the ⟨100⟩ directions, which explains the larger residual deformation observed in these directions. The decrease of the difference between the residual deformation along two directions with increasing thickness is connected to the fact that, when the average film thickness increases, a smaller fraction is in the form of islands and the islands are flatter, resulting in a decrease of the fraction of the film located near island edges. Therefore, the fraction of the film that may relax due to deformation of the island edges is smaller, and the deformation tends to be more biaxial. These considerations also show that part of the deviation from the theoretical residual deformation value could be due to a partial 3D character of the film, which is a function of thickness.

For Ag thicknesses of 1300 Å and 1500 Å, SEM investigations clearly showed that the films are continuous, excepted for a small fraction of holes running through the whole thickness. The residual deformation should then be purely biaxial, which is our experimental observation. Large differences between the experimental and calculated residual deformations are, however, found after annealing. The experimental residual deformations are also found to depend on the substrate step density.

Before discussing this effect, we need to evaluate the return force exerted on a dislocation that is slightly displaced with respect to its equilibrium position in the direction parallel to the interface. This was done by using the Peierls-Nabarro model.[32] The lateral return force on a dislocation displaced by one atomic plane with respect to its equilibrium CSL position was found to be of the order of $8\times10^{-4}\mu_{Ag}$, only slightly smaller than the critical gliding strain of $4\times10^{-3}\mu_{Ag}$. The gliding of interfacial dislocations should be even easier, since the Ag-O binding energy is much smaller than the Ag-Ag one.[2] Therefore, the interfacial dislocations can not be displaced from their equilibrium position by more than a few atomic distances, unless they are pinned by interfacial defects such as steps. This is in good agreement with the experimental result that the average dislocation spacing is always the equilibrium one when increasing the temperature, i.e., when decreasing the misfit. This calculation shows in addition that large fluctuations of the separation between dislocations around the average value are very unlikely, which is an important result for the following discussion.

For all thick samples, during anneals at progressively increasing temperatures, the misfit was found to behave as expected from the respective thermal expansion coefficients of Ag and MgO. By contrast, smaller misfits are always found for decreasing temperatures, and, whatever the highest tem-

perature that has been reached, the difference in lattice parameters back to RT is smaller after annealing than before.

For all miscut samples, the position (measured at RT) of the Ag peaks is $h_{Ag}=2.058\pm0.001$ after high-temperature annealing, compared to 2.061 before annealing. This difference corresponds to a lattice parameter misfit of $2.82\pm0.05\%$, i.e., a residual deformation of $+0.16\%$ in silver. This residual deformation is by far larger than the theoretical elastic deformation for 1500-Å-thick films. The Ag film is also constrained perpendicular to the interface: the location of the Ag(002) Bragg peak yields a $-0.25\%$ contraction, which is the value expected from the linear elasticity theory with a $+0.16\%$ expansion parallel to the surface.

On the flat sample, the residual deformation after high-temperature annealing is even larger: $h_{Ag}=2.055\pm0.001$, which corresponds to a misfit of $2.75\pm0.05\%$, or to a residual deformation of $0.31\pm0.05\%$, roughly double that observed on miscut samples.

It is possible to show[22] that this phenomenon cannot be explained by misfit relaxation resulting from stacking faults. The relaxation is thus likely to be fully realized by misfit edge dislocations. With this assumption, the linear dislocation density $n$ in the $\langle 110\rangle$ direction is directly related to the misfit parameter $f$. We find that 5.5% and 7.9% of dislocations are ''lacking'' on the miscut and flat samples, respectively, after the annealing cycle. There is thus a clear correlation between the substrate step density and the residual deformation after annealing.

Let us first consider the flat substrate, with no pinning centers. For a completely relaxed Ag film at RT, $f=-2.98\%$ yields a linear dislocation density along the $\langle 110\rangle$ direction of $n=103$ dislocations/$\mu$m, while at 800 °C, $f\sim-2.5\%$ yields $n=86$ dislocations/$\mu$m, i.e., 17% less than at RT. The distance between dislocations is then 6 to 7 (110) atomic planes larger at 800 °C, and thus corresponds to a significant displacement of these dislocations with respect to their RT position. Since the gliding motion is easy in the (001) plane, and since the dislocations cannot be displaced from their equilibrium position by more than one or two interatomic distances, the excess dislocations must be eliminated at the edges of the Ag islands or of the Ag film upon heating. During cooling, new dislocations must have nucleated, as shown by the larger misfit after cooling (2.75%) than at high temperature (2.5%). Since the gliding plane is the interface plane, this introduction must proceed at the edges of islands or of the silver film.

When steps are present, they act as pinning centers because, in order to cross a step, a dislocation has to undergo a climb, which is only possible with the addition of new atoms. This process requires atomic diffusion, and is thus much less favored than simple dislocation gliding. Since the substrate steps pin the dislocations, the larger the step density, the smaller the number of dislocations that are eliminated at high temperature. The excess dislocations must then stay on their terrace. They should not stay pinned by the steps, since in that case, the residual deformation should increase with the step density, which is contrary to the experimental observation. On a given terrace, fully covered by silver, it is thus likely that the total number of dislocations remains constant. Hence, the larger the step density, the less the number of dislocations that have to be reintroduced during cooling, because steps are a reservoir of dislocations.

We thus find that, the larger the number of dislocations that have to be reintroduced during cooling, the larger the residual deformation. This can only be explained by the existence of a barrier to the nucleation of new dislocations.

This conclusion in turn provides important information concerning the initial formation of interfacial dislocations during growth. Indeed, on all 1500-Å-thick as-grown samples, the Ag film was fully relaxed. This implies (still in the hypothesis that only the $a/2[110]$ dislocations participate to the misfit relaxation) that the introduction of dislocations is a progressive process during growth, rather than a simple nucleation followed by gliding, because in the latter case, a significant residual deformation should be observed. It is likely that dislocations are naturally introduced at the edges of growing islands when they reach a critical lateral size equal to the period $\Lambda$ of the CSL.

## VI. CONCLUSIONS

This study of thick Ag epilayers on MgO(001) by grazing incidence x-ray diffraction has confirmed the existence of an ordered network of interfacial misfit dislocations. These dislocations were found to have pure edge character, oriented along the common $\langle 110\rangle$ directions of the film and the substrate, with $\frac{1}{2}[110]$ Burgers vectors in the Ag lattice. The dislocations are separated by 97 Å on the as-grown films, which is in agreement with the coincident site lattice formed in the case of only one kind of site for the epitaxy of Ag on MgO(001). This result is in contradiction with the conclusion of a previous HRTEM study, which probably suffered from the difficulty to prepare the samples in this system. It demonstrates the power of GIXS to analyze ordered, buried interfaces in a nondestructive way.

The presence of growth faults, in particular stacking faults and twins in the silver film, has also been detected. The density of stacking faults is linked to the quality of the substrate surface, in particular the step density.

During annealing, the Ag crystalline quality drastically improves, with a reduction of the mosaic spread by a factor 2.5. In addition, new satellites of diffraction by the dislocation network become measurable. It was then possible to quantitatively analyze the diffraction pattern by use of a model of the dislocation network based on the linear elasticity theory in a continuous and isotropic medium. A good agreement with the experimental data is obtained, which shows that the substrate is deformed according to the elastic predictions, and that no intermediate layer is needed to account for the weak Ag-O bond at the interface.

The period of the dislocation network adapts itself to the lattice parameter misfit at all temperatures investigated, and no kinetic evolution could be detected, at least at the time scale of the experiment. It would be interesting to design experiments that would allow one to separate between the kinetic effects and the driving force effect, which is the instantaneous thermal expansion pulling the dislocations out of their equilibrium positions. One way would be to compare measurements performed at room temperature and below, in a temperature range where the atomic diffusion is very slow and can thus be neglected.

A large residual deformation is systematically found after annealing, which is linked to the density of steps on the substrate. This shows the existence of a barrier to the nucleation of misfit dislocations in a continuous film. A consequence is that the misfit dislocations that are present in thick Ag films on MgO(001) after growth are likely to form during the growth at the edge of islands, rather than after a constrained, continuous film has reached a critical thickness.

**ACKNOWLEDGMENTS**

We are very indebted to Professor P. Flynn and Dr. M.-H. Yang, of the Materials Research Laboratory, University of Illinois, Urbana, Illinois, for their kind elaboration and provision of most of the samples studied. We would also like to thank A. Bourret, O. Robach, and Jany Thibault-Dessault for valuable discussions, and B. Villette for efficient help during the first experiments performed at LURE.

*Author to whom correspondence should be addressed. Present address: CEA-Grenoble, Département de Recherche Fondamentale sur la Matière Condensée/SP2M/IRS, 17, rue des Martyrs, 38054 Grenoble Cédex 9, France. FAX: (33) 4 76 88 51 38. Electronic address: grenaud@cea.fr

[1] For a review, see *Metal-Ceramic Interfaces*, edited by M. Rühle, A. G. Evans, M. F. Ashby, J. P. Hirth (Pergamon Press, New York, 1990); Proceedings of the International Symposium on Metal-Ceramic Interfaces [Acta Metall. Mater. **40**, (1992)].

[2] A. M. Stoneham and P. W. Tasker, J. Phys. C **18**, L543 (1985); M. W. Finnis, Acta Metall. Mater. **40**, S25 (1992); U. Schönberger, O. K. Andersen, M. Methfessel, *ibid.* **40**, S1 (1992); J. R. Smith, T. Hong, D. J. Srolovitz, Phys. Rev. Lett. **72**, 4021 (1994).

[3] J. H. van der Merwe, Philos. Mag. A **45**, 127 (1982); **45**, 145 (1982); **45**, 159 (1982).

[4] T. Epicier and C. Esnouf, J. Phys. III **4**, 1811 (1994).

[5] R. H. Hoel, H.-U. Habermeier, and M. Rühle, J. Phys. (Paris), Colloq. **46**, C4-141 (1989); R. H. Hoel, Surf. Sci. **169**, 317 (1986); R. H. Hoel, J. M. Penisson, and H. U. Habermeier, J. Phys. (Paris), Colloq. **51**, C1-837 (1989).

[6] F. Ernst, P. Pirouz, and A. H. Heuer, Philos. Mag. A **63**, 259 (1991).

[7] G. Necker and W. Mader, Philos. Mag. Lett. **58**, 205 (1988).

[8] A. Trampert, F. Ernst, C. P. Flynn, H. F. Fischmeister, and M. Rühle, Acta Metall. Mater. **40**, S227 (1992).

[9] P. Guénard, G. Renaud, and B. Villette, Physica B **221**, 205 (1996).

[10] For a review on GIXS, see, for instance, I. K. Robinson and D. J. Tweet, Rep. Prog. Phys. **55**, 599 (1992).

[11] A. Bourret and J. Thibault-Dessault (private communication).

[12] A. Bourret and P. H. Fuoss, Appl. Phys. Lett. **61**, 1034 (1992).

[13] H. Grimmer, W. Bollmann, and D. H. Warrington, Acta Crystallogr., Sect. A: Cryst. Phys., Diffr., Theor. Gen. Crystallogr. **30**, 197 (1974).

[14] W. Bollmann, *Crystal Defects and Crystalline Interfaces* (Springer, Berlin, 1970).

[15] C. P. Flynn and S. Yadavalli, Acta Metall. Mater. **40**, S45 (1992).

[16] C. P. Flynn, J. Phys. F **18**, L195 (1988).

[17] O. Robach, G. Renaud, and A. Barbier, Surf. Sci. **401**, 227 (1998).

[18] O. Robach, G. Renaud, A. Barbier, and P. Guénard, Surf. Rev. Lett. **5**, 359 (1998).

[19] G. Renaud, B. Villette, and P. Guénard, Nucl. Instrum. Methods Phys. Res. B **95**, 422 (1995).

[20] ESRF beamline handbook and http://www.esrf.fr

[21] S. R. Andrews and R. A. Cowley, J. Phys. C **18**, 6247 (1985); I. K. Robinson, Phys. Rev. B **33**, 3830 (1986).

[22] P. Guénard, Ph.D. thesis, Grenoble University, 1996.

[23] M. S. Patterson, J. Appl. Phys. **8**, 805 (1952).

[24] *Handbook of Thermophysical Properties of Solid Materials*, Vol. 3, edited by A. Goldsmith, T. E. Waterman, and H. J. Hirschhorn (MacMillan, New York, 1961).

[25] G. Renaud, O. Robach, and A. Barbier (unpublished); O. Robach, Ph.D. thesis, Grenoble University, 1997.

[26] J. Dundurs, G. P. Sendeckyj, J. Appl. Phys. **36**, 3353 (1965).

[27] W. Mader and D. Knauss, Acta Metall. Mater. **40**, S207 (1992).

[28] R. Bonnet and J. L. Verger-Gaugry, Philos. Mag. A **66**, 849 (1992).

[29] R. Bonnet, Philos. Mag. A **43**, 1165 (1981).

[30] C. A. B. Ball, Phys. Status Solidi **42**, 357 (1970).

[31] J. W. Matthews, D. C. Jackson, and A. Chambers, Thin Solid Films **26**, 129 (1975).

[32] J. Friedel, *Dislocations* (Pergamon Press, New York, 1964).